Published in final edited form as:
Transl Stroke Res. 2013 October 1; 4(5): . doi:10.1007/s12975-013-0270-5.

Deferoxamine reduces neuronal death and hematoma lysis after intracerebral hemorrhage in aged rats

Tetsuhiro Hatakeyama, MD[1,2], **Masanobu Okauchi, MD**[1,2], **Ya Hua, MD**[1], **Richard F. Keep, PhD**[1], and **Guohua Xi, MD**[1]

[1]Department of Neurosurgery, University of Michigan, USA

[2]Department of Neurological Surgery, Kagawa University, Japan

Abstract

Intracerebral hemorrhage (ICH) is primarily a disease of the elderly. Deferoxamine (DFX), an iron chelator, reduces long-term neurological deficits and brain atrophy after ICH in aged rats. In the present study, we investigated whether DFX can reduce acute ICH-induced neuronal death and whether it affects the endogenous response to ICH (ferritin upregulation and hematoma resolution) in aged rats. Male Fischer 344 rats (18 months old) had an intracaudate injection of 100 μL autologous whole blood into the right basal ganglia and were treated with DFX (100 mg/kg) or vehicle 2 hours post-ICH and then every 12 hours up to 7 days. Rats were euthanized 1, 3, or 7 days later for neuronal death, ferritin and hematoma size measurements. Plasma ferritin levels and behavioral outcome following ICH were also examined. DFX treatment significantly reduced ICH-induced neuronal death and neurological deficits. DFX also suppressed ferritin upregulation in the ipsilateral basal ganglia after ICH and hematoma lysis (hematoma volume at day 7: 13.2±4.9 vs. 3.8±1.2 mm^3 in vehicle-treated group, $p < 0.01$). However, effects of DFX on plasma ferritin levels after ICH did not reach significance. In conclusion, DFX reduces neuronal death and neurological deficits after ICH in aged rats. It also affects the endogenous response to ICH.

Keywords

Cerebral hemorrhage; deferoxamine; iron; neuronal death

Introduction

Erythrocyte lysis and iron toxicity contribute to brain injury after intracerebral hemorrhage (ICH) (1–7). Previous studies have found that deferoxamine (DFX), an iron chelator, reduces ICH- or hemoglobin-induced brain edema, neuronal death, neurological deficits, and brain atrophy in young rats (1, 8–12). ICH is, though, mainly a disease of the elderly(13), and aging is an important factor affecting brain injury after ICH. We have, therefore, been examining the effects of DFX in aged animals. Our recent study found that DFX reduces long-term behavioral deficits and brain atrophy after ICH in aged rats(14). The current study examines the effects of DFX on acute ICH-induced neuronal death.

Correspondence and Reprint Request: Guohua Xi, M.D., R5018, BSRB, University of Michigan, 109 Zina Pitcher Place, Ann Arbor, Michigan 48109-2200, Tel: 734-764-1207, Fax: 734-763-7322, guohuaxi@umich.edu.

Disclosures
None

Conflict of Interest:
Tetsuhiro Hatakeyama, Masanobu Okauchi, Ya Hua, Richard F. Keep and Guohua Xi declare that they have no conflict of interest.

In addition, it is uncertain how DFX treatment affects the endogenous response to ICH. Ferritin, a naturally occurring iron chelator, is involved in maintaining iron homeostasis in the brain. This protein is composed of two subunit types: the heavy (H)- and light (L)-chains that assemble in various proportions to form spherical shells of 24 subunits(15). The H- and L-chains have distinct functions: the H-chain has ferroxidase activity, while the L-chain assists the H-chain in hybrid molecules increasing the efficiency of iron nucleation(16). In ICH patients, serum ferritin level correlates with perihematoma edema volume and with poor outcome (17, 18). The current study examines whether treatment with DFX may affect the response of this endogenous iron chelator to ICH.

Another endogenous response to ICH is the activation of mechanisms that clear the hematoma. This study examines whether DFX treatment affects that clearance.

Materials and Methods

Animal Preparation and Intracerebral Infusion

Animal use protocols were approved by the University of Michigan Committee on the Use and Care of Animals. A total of 78 aged male Fischer 344 rats (18-month old; weight, 410–560 g; NIH) were used in this study. Rats were anesthetized with pentobarbital (45 mg/kg, i.p.). The right femoral artery was catheterized for continuous blood pressure monitoring and blood sampling. Blood was obtained from the catheter for analysis of blood pH, PaO_2, $PaCO_2$, hematocrit, and blood glucose. Core temperature was maintained at 37°C with use of a feedback-controlled heating pad. Rats were positioned in a stereotactic frame (Kopf Instruments), and a cranial burr hole (1 mm) was drilled on the right coronal suture 3.5 mm lateral to the midline. A 26-gauge needle was inserted stereotactically into the right basal ganglia (coordinates: 0.2 mm anterior, 5.5 mm ventral, 3.5 mm lateral to the bregma). Autologous whole blood (100 μL) was injected at a rate of 10 μL/minute using a microinfusion pump. In sham-operated animals 100 μL saline was infused. After injection, the needle was removed, the burr hole was filled with bone wax, and the skin incision was closed with sutures.

Experimental Groups

Rats had ICH or saline control and received either DFX (100 mg/kg administered intramuscularly, 2 h after infusion of 100 μL autologous blood and then at 12-h intervals for up to 7 days) or vehicle (the same amount of saline) treatment. Rats were divided into three sets. In the first set, rats received either an intracerebral infusion of 100 μL autologous blood (ICH, n = 5 each group) or an infusion of 100 μL saline (control, n = 3 each group), and then received either DFX treatment or vehicle (the same amount of saline) treatment. The ICH rats were killed 1, 3 and 7 days later, and the saline-control rats were killed at 7 days, for histological examination. In the second set, rats (n = 4 each group) received an intracerebral infusion of 100 μL autologous blood, and then received either DFX or vehicle. Rats were killed at 1, 3 and 7 days for Western blot analysis. In the third set, rats (n = 9 each group) received an intracerebral infusion of 100 μL autologous blood and then received either DFX or vehicle. All animals underwent behavioral testing. Plasma ferritin levels were measured at days 1, 3 and 7.

Western blot analysis

Rats were anesthetized and underwent intracardiac perfusion with 0.1 mol/L. phosphate-buffered saline (pH 7.4). Brains were removed and a 3-mm-thick coronal brain slice cut approximately 4 mm from the frontal pole. The slice was separated into ipsi- and contralateral basal ganglia. Western blot analysis was performed as previously described(19). Protein concentration was determined using a Bio-Rad Laboratories

(Hercules, CA, USA) protein assay kit. Fifty μg protein from each sample was separated by sodium dodecyl sulfate-polyacrylamide gel electrophoresis (SDS-PAGE) and transferred to a hybond-C pure nitrocellulose membrane (Amersham, Piscataway, NJ, USA). Membranes were blocked in Carnation nonfat milk and probed with primary and secondary antibodies. The primary antibodies were rabbit anti-FTH1 antibody (H-chain; Cell Signaling Technology, Beverly, MA, USA; 1:2000), polyclonal goat anti-FTL antibody (L-chain; Abnova, Walnut, CA, USA, 1:2000) and monoclonal mouse anti-beta-actin antibody (Sigma, USA, 1:2000). The secondary antibodies were goat anti-rabbit IgG, rabbit anti-goat IgG and goat anti mouse IgG (each 1:2500; Bio-Rad Laboratories). The antigen-antibody complexes were visualized with a chemiluminescence system (Amersham, Piscataway, NJ, USA) and exposed to a Kodak X-OMAT film (Rochester, NY, USA). Relative densities of bands were analyzed with the NIH Image program (Version 1.62, Bethesda, MD, USA).

Immunohistochemistry

Immunohistochemistry was performed as described previously(20, 21). Rats were anesthetized (pentobarbital, 60 mg/kg i.p.) and underwent transcardiac perfusion with 4% paraformaldehyde in 0.1 mol/L phosphate-buffered saline (pH 7.4). Brains were removed, kept in 4% paraformaldehyde for 6 hours, and then immersed in 30% sucrose for 3–4 days at 4°C. Brains were then placed in optimal cutting temperature embedding compound (Sakura Finetek, Inc.) and sectioned on a cryostat (18-μm thick slices). Immunohistochemistry staining was performed using the avidin-biotin complex technique. The primary antibody was polyclonal rabbit anti-human ferritin IgG (Sigma-Aldrich, St. Louis, MO, USA; 1:300) and the secondary was biotinylated goat anti-rabbit IgG (Bio-Rad Laboratories, 1:500). Normal rabbit IgG was used as a negative control.

Terminal dUDP nick end labeling (TUNEL) staining

TUNEL staining was performed to assess DNA fragmentation using an ApopTag® Peroxidase In Situ Apoptosis Detection Kit (Millipore, Billerica, MA, USA).

Fluoro-Jade C staining

Fluoro-Jade staining was used to assess neuronal degeneration(22). Sections were rinsed in basic alcohol for 5 min, followed by a 2 min rinse in 70% alcohol. Sections were then briefly rinsed in distilled water and incubated in 0.06% $KMnO_4$ for 10 min. Sections were then briefly rinsed in distilled water to remove excess $KMnO_4$ and incubated in 0.0001% Fluoro-Jade C stain in 0.1% acetic acid for 10 min. Following Fluoro-Jade C labeling, sections were rinsed three times in distilled water, air dried for 10 min and cleared in xylene and cover slipped with DPX.

Cell Counting

To assess the effects of DFX on neuronal death and DNA damage, we used 18-μm-thick coronal sections from 1-mm posterior to the blood injection site. High-power images (x40 magnification) were taken from the caudate using a digital camera. Fluoro-Jade C and TUNEL positive cells were counted. Counts were performed on 4 areas in each brain section.

Plasma ferritin

Rats were anesthetized with pentobarbital. Plasma was obtained (transcardiac) at 1, 3 and 7 days after ICH and stored at −80 °C before determination. Ferritin levels were determined by ELISA using a Rat Ferritin ELISA Kit (Immunology Consultants Lab, Newberg, OR, USA).

Hematoma volume

Hematoma volume was determined using well-established procedures(23, 24). Frozen brain sections from animals euthanized 1 day, 3 days and 7 days after ICH onset were taken every 200 μm, starting at +2 mm to bregma and extending to −4 mm to bregma. The sections were stained with hematoxlin-eosin and scanned. The hematoma was outlined for area measurement using Image J. All measurements were repeated 3 times and the mean value was used to determine hematoma volume.

Behavioral Tests

For behavioral tests, all animals were tested before and after surgery and scored by experimenters who were blind to treatment group (21). The following tests were used.

(A) Forelimb-Placing Test—Forelimb placing was scored using a vibrissae-elicited forelimb placing test. Independent testing of each forelimb was induced by brushing the vibrissae ipsilateral to that forelimb on the edge of a tabletop once per trial for 10 trials. Intact animals placed the forelimb quickly onto the countertop. Percentage of successful placing responses was determined. There is a reduction in successful responses in the forelimb contralateral to the site of injection after ICH.

(B) Corner Turn Test—Rats were allowed to proceed into a 30° corner. To the exit the corner, the rat could turn either left or right, and the direction was recorded. This task was repeated 10 to 15 times and the percentage of right turns calculated.

Statistical Analysis

In this study, all data are presented as means±SD. Data were analyzed with Student's t-test or Kruskal-Wallis Test. Differences were considered significant at $P<0.05$.

Results

Mortality

Mortality rate was low in aged rats after ICH. Two of 72 ICH rats died during the experiments. One rat was treated with vehicle and the other was treated with deferoxamine.

Neuronal death

Neuronal death in the perihematomal area was detected by Fluoro-Jade C staining (Fig. 1). At day 1 after ICH, the number of Fluoro-Jade C positive cells was significantly decreased in the DFX-treated group (258 ± 51 vs. 375 ± 90/mm^2 in vehicle-treated group, $p<0.05$). By day 3, the number of Fluor-Jade C positive cells in the vehicle-treated group decline and there was no difference between DFX- and vehicle-treated groups. However, Fluoro-Jade C was not sensitive at detecting neuronal death at day 7 following ICH with few positive cells detected around the hematoma in both DFX-treated group and vehicle-treated group at that time point.

DNA damage

DNA damage in the perihematomal area was detected by TUNEL staining (Fig. 2). At day 1, the number of TUNEL positive cells was significantly decreased in the DFX-treated group (133 ± 88 vs. 294 ± 54/mm^2 in vehicle-treated group, $P<0.05$). Again, there were no differences between DFX and vehicle treatment at day 3.

Neurological deficits

Forelimb-placing and the corner turn tests, were performed 1, 3 and 7 days after ICH. In vehicle treated rats, there was little recovery of forelimb-placing with time. In the DFX treated-group, there was a significant recovery compared to vehicle-treatment at day 7 (25 ± 16.6 % vs. 2 ± 4 % response rate in vehicle-treated group, $P<0.01$; Fig. 3A). In the corner turn test, the percentage of turns to the right was significantly decreased at day 3 and 7 in DFX-treated group compared with vehicle-treated group (85 ± 11 % vs. 95 ± 7 % in vehicle-treated group at day 3, $p< 0.05$; 78 ± 12 % vs. 90 ± 8 % in vehicle-treated group at day 7, $p<0.05$; Fig. 3B).

Hematoma resolution

Hematoma volume was assessed at days 1, 3 and 7 (Fig. 4). There was no significant difference in the hematoma volume between vehicle- and DFX-treated groups at days 1 and 3. However, hematoma resolution was significantly reduced in the DFX-treated group at day 7 (13.2 ± 4.9 vs. 3.8 ± 1.2 mm^3 in vehicle-treated group, $p<0.01$).

Upregulation of ferritin

Endogenous ferritin has an important role in iron chelation after ICH. After ICH, there was a progressive increase in both H- and L-chain protein levels in the ipsilateral basal ganglia with time (Fig. 5). DFX suppressed this upregulation (Fig. 6). Thus, as assessed by Western blot, ferritin H-chain was reduced by DFX treatment (2437±487 vs. 3393±343 pixels in vehicle-treated group, $p<0.05$) as was the L-chain (2081±411 vs. 3375±497 pixels in vehicle-treated group, $p<0.05$).

Plasma ferritin level

Plasma ferritin levels were measured by ELISA. In vehicle-treated rats, plasma ferritin levels in ICH animals (559 ± 439 ng/ml) were significantly higher than in rats injected with saline (180 ± 9 ng/ml, $p<0.05$) at day 7. There was a trend for plasma ferritin levels at day 3 and day 7 after ICH to be lower with DFX compared to vehicle treatment (day 3: 282 ± 62 vs. 630 ± 730 ng/ml with vehicle; day 7: 335 ± 79 vs. 559 ± 439 ng/ml with vehicle), but these differences did not reach significance.

Discussion

In an animal model of aging, DFX treatment attenuated ICH-induced acute neuronal death and neurological deficits suggesting that iron chelation therapy may be a useful therapy for patients with ICH in acute stage. DFX also affected the endogenous response to ICH, suppressing ferritin upregulation and slowing hematoma resolution in aged rats. However, it is difficult to examine the effect of DFX on ICH-induced mortality in the blood injection model because ICH results in very low mortality in both young and aged rats.

We chose to inject DFX at a dose of 100 mg/kg because our previous study showed that this dose was effective in reducing ICH-induced brain injury in young and aged rat models(8, 9, 14). The therapeutic time window and optimal duration is also based on our previous study(25). The average lifespan of people is 72 years and the average lifespan of a male rat is between 2 and 3 years. As a percent of average lifespan, 18 months old in a rat corresponds to 50 years old in a human.

Oxidative brain injury and apoptotic cell death occur in brain after intracerebral infusion of autologous blood(10, 26, 27). Iron-induced brain damage may result from oxidative stress(4) and free iron can stimulate the formation of free radicals leading to neuronal damage. DNA is vulnerable to oxidative stress. DNA damage by reactive oxygen species can be greatly

amplified in the presence of free iron(28). DFX, an iron chelator, is approved by FDA for treatment of acute iron intoxication and chronic iron overload in transfusion-dependent anemia. Its molecular weight is 657, and DFX can rapidly penetrate the blood-brain barrier and accumulate in brain tissue at a significant concentration after systemic administration(29, 30). We have previously reported that systemic DFX attenuates brain edema in rats after intracerebral infusion of autologous whole blood or hemoglobin (1, 9). In the present study, we found that the number of Fluoro-Jade C and TUNEL positive cells peaked at day 1 after ICH and DFX reduced these cells at that time point in aged rats. These results indicate that DFX may reduce neuron death in the aged rat ICH model.

In animal models of stroke, the inclusion on a behavioral investigation and the data derived from it represents an important step forward, because a potential therapeutic compound should have a positive effect on behavior and function after stroke. We have used several sensorimotor behavioral tests to examine ICH-induced neurological deficits(21). Here, DFX improved both forelimb placing and corner turn scores in aged rats.

After ICH there is the induction of a number of mechanisms that may limit brain injury. Ferritin, a naturally occurring iron chelator, is involved in maintaining brain iron homeostasis, and the brain can produce ferritin. Ferritin has 2 subunits: ferritin H-chain, which is related to iron utilization, and ferritin L-chain, which is associated with iron storage(31). Ferritin protein synthesis is regulated mostly post-transcriptionally by iron-mediated or non-iron-mediated induction(32) and an upregulation in brain ferritin level may be neuroprotective. Our present data found that brain ferritin levels (H- and L-chains) increased progressively after ICH and DFX-treatment significantly reduced brain ferritin levels at day 7 in aged rats. These results suggest that DFX may reduce iron overload in the aged rat ICH model, thereby reducing ferritin induction. In addition, DFX has a marked effect on neuronal death at day 1 after ICH, before there is maximal ferritin upregulation, suggesting that one of the protective actions of DFX is chelation of early iron-release from the hematoma.

In a clinical study, high-serum ferritin levels are correlated with poor outcome in patients with ICH(33) and there is also a positive correlation between serum ferritin and relative perihematoma edema volume in patients with ICH(17). In the current study, we showed that ICH increased plasma ferritin levels compared to saline injection 7 days after surgery. These results suggest that iron from the hematoma may be released into general circulation resulting in systemic ferritin upregulation. Although there was a tendency for DFX to reduce plasma ferritin levels at 3 and 7 days after ICH (~50%), this did not reach significance. Further studies are required to identify the mechanisms upregulating plasma ferritin level after ICH.

Clot resolution in the rat(34, 35) and human(35, 36) takes days to weeks and there may be a gradual release of iron over that period. Aged rats have more fragile erythrocytes, leading to easier hemolysis after ICH(37). Our previous study showed that the duration over which clot lysis and iron release occur are likely to be dependent on clot size (i.e. 1 to 3 days for an 100 μL clot in rats and 3 to 7 days for a 2.5 mL clot in pigs), and DFX is effective in reducing injury in models with different sized clots(38). The current study found that DFX-treatment reduces the rate of hematoma clearance in the aged rat (greater residual hematoma volume at day 7). The underlying mechanism is still uncertain, but there is evidence that DFX can inhibit hemin-induced erythrocyte lysis(39). Alternately, it may affect macrophage activity which is involved in hematoma clearance. This merits further study. This is particularly the case because hematoma volume correlates with poorer outcome in humans(40, 41) and therapies that promote hematoma clearance improve functional outcome in animal studies(42). The current study is a case of an agent slowing hematoma resolution but

improving outcome. The effects of DFX on injury do not appear to be via a delay in injury, as it improves chronic as well as acute outcome in rats after ICH (14, 25).

In summary, systemic administration of DFX reduced ICH-induced acute neuronal death and neurological deficits in aged rats suggesting that DFX may reduce brain injury in ICH patients. DFX also suppressed the endogenous response to ICH, suppressing an upregulation of the endogenous iron chelator ferritin and reducing the rate of hematoma clearance.

Acknowledgments

This study was supported by grants NS-052510, NS-057539, NS-073595 and NS-079157 from the National Institutes of Health (NIH). The content is solely the responsibility of the authors and does not necessarily represent the official views of the NIH.

References

1. Huang FP, Xi G, Keep RF, Hua Y, Nemoianu A, Hoff JT. Brain edema after experimental intracerebral hemorrhage: role of hemoglobin degradation products. J Neurosurg. 2002 Feb; 96(2): 287–93. [PubMed: 11838803]
2. Wagner KR, Dwyer BE. Hematoma removal, heme, and heme oxygenase following hemorrhagic stroke. Ann N Y Acad Sci. 2004 Mar.1012:237–51. [PubMed: 15105270]
3. Wagner KR, Sharp FR, Ardizzone TD, Lu A, Clark JF. Heme and iron metabolism: role in cerebral hemorrhage. J Cereb Blood Flow Metab. 2003 Jun; 23(6):629–52. [PubMed: 12796711]
4. Wu J, Hua Y, Keep RF, Schallert T, Hoff JT, Xi G. Oxidative brain injury from extravasated erythrocytes after intracerebral hemorrhage. Brain Res. 2002 Oct 25; 953(1–2):45–52. [PubMed: 12384237]
5. Xi G, Keep RF, Hoff JT. Erythrocytes and delayed brain edema formation following intracerebral hemorrhage in rats. J Neurosurg. 1998 Dec; 89(6):991–6. [PubMed: 9833826]
6. Rincon F, Mayer SA. Intracerebral Hemorrhage: CLinical Overview and Pathophysiologic Concepts. Transl Stroke Res. 2012; 3(Suppl 1):s10–s24.
7. Bodmer D, Vaughan KA, Zacharia BE, Hickman ZL, Connolly ES Jr. The Molecular Mechanisms that Promote Edema After Intracerebral Hemorrhage. Transl Stroke Res. 2012; 3(suppl 1):s52–s61.
8. Hua Y, Nakamura T, Keep RF, Wu J, Schallert T, Hoff JT, et al. Long-term effects of experimental intracerebral hemorrhage: the role of iron. J Neurosurg. 2006 Feb; 104(2):305–12. [PubMed: 16509506]
9. Nakamura T, Keep RF, Hua Y, Schallert T, Hoff JT, Xi G. Deferoxamine-induced attenuation of brain edema and neurological deficits in a rat model of intracerebral hemorrhage. J Neurosurg. 2004 Apr; 100(4):672–8. [PubMed: 15070122]
10. Nakamura T, Keep RF, Hua Y, Hoff JT, Xi G. Oxidative DNA injury after experimental intracerebral hemorrhage. Brain Res. 2005 Mar 28; 1039(1–2):30–6. [PubMed: 15781043]
11. Song S, Hua Y, Keep RF, Hoff JT, Xi G. A new hippocampal model for examining intracerebral hemorrhage-related neuronal death: effects of deferoxamine on hemoglobin-induced neuronal death. Stroke. 2007 Oct; 38(10):2861–3. [PubMed: 17761912]
12. Keep RF, Hua Y, Xi G. Intracerebral haemorrhage: mechanisms of injury and therapeutic targets. Lancet Neurol. 2012 Aug; 11(8):720–31. [PubMed: 22698888]
13. Collins TC, Petersen NJ, Menke TJ, Souchek J, Foster W, Ashton CM. Short-term, intermediate-term, and long-term mortality in patients hospitalized for stroke. J Clin Epidemiol. 2003 Jan; 56(1):81–7. [PubMed: 12589874]
14. Okauchi M, Hua Y, Keep RF, Morgenstern LB, Xi G. Effects of deferoxamine on intracerebral hemorrhage-induced brain injury in aged rats. Stroke. 2009 May; 40(5):1858–63. [PubMed: 19286595]
15. Harrison PM, Arosio P. The ferritins: molecular properties, iron storage function and cellular regulation. Biochim Biophys Acta. 1996 Jul 31; 1275(3):161–203. [PubMed: 8695634]

16. Arosio P, Levi S. Ferritin, iron homeostasis, and oxidative damage. Free Radic Biol Med. 2002 Aug 15; 33(4):457–63. [PubMed: 12160928]

17. Mehdiratta M, Kumar S, Hackney D, Schlaug G, Selim M. Association between serum ferritin level and perihematoma edema volume in patients with spontaneous intracerebral hemorrhage. Stroke. 2008 Apr; 39(4):1165–70. [PubMed: 18292378]

18. Perez de la Ossa N, Sobrino T, Silva Y, Blanco M, Millan M, Gomis M, et al. Iron-related brain damage in patients with intracerebral hemorrhage. Stroke. 2010 Apr; 41(4):810–3. [PubMed: 20185788]

19. Xi G, Keep RF, Hua Y, Xiang J, Hoff JT. Attenuation of thrombin-induced brain edema by cerebral thrombin preconditioning. Stroke. 1999 Jun; 30(6):1247–55. [PubMed: 10356108]

20. Hua Y, Xi G, Keep RF, Wu J, Jiang Y, Hoff JT. Plasminogen activator inhibitor-1 induction after experimental intracerebral hemorrhage. J Cereb Blood Flow Metab. 2002 Jan; 22(1):55–61. [PubMed: 11807394]

21. Hua Y, Schallert T, Keep RF, Wu J, Hoff JT, Xi G. Behavioral tests after intracerebral hemorrhage in the rat. Stroke. 2002 Oct; 33(10):2478–84. [PubMed: 12364741]

22. Schmued LC, Albertson C, Slikker W Jr. Fluoro-Jade: a novel fluorochrome for the sensitive and reliable histochemical localization of neuronal degeneration. Brain Res. 1997 Mar 14; 751(1):37–46. [PubMed: 9098566]

23. Wasserman JK, Yang H, Schlichter LC. Glial responses, neuron death and lesion resolution after intracerebral hemorrhage in young vs. aged rats. Eur J Neurosci. 2008 Oct; 28(7):1316–28. [PubMed: 18973558]

24. MacLellan CL, Silasi G, Poon CC, Edmundson CL, Buist R, Peeling J, et al. Intracerebral hemorrhage models in rat: comparing collagenase to blood infusion. J Cereb Blood Flow Metab. 2008 Mar; 28(3):516–25. [PubMed: 17726491]

25. Okauchi M, Hua Y, Keep RF, Morgenstern LB, Schallert T, Xi G. Deferoxamine treatment for intracerebral hemorrhage in aged rats: therapeutic time window and optimal duration. Stroke. 2010 Feb; 41(2):375–82. [PubMed: 20044521]

26. Nakamura T, Xi G, Park JW, Hua Y, Hoff JT, Keep RF. Holo-transferrin and thrombin can interact to cause brain damage. Stroke. 2005 Feb; 36(2):348–52. [PubMed: 15637325]

27. Xi G, Keep RF, Hoff JT. Mechanisms of brain injury after intracerebral haemorrhage. Lancet Neurol. 2006 Jan; 5(1):53–63. [PubMed: 16361023]

28. Aruoma OI, Halliwell B, Dizdaroglu M. Iron ion-dependent modification of bases in DNA by the superoxide radical-generating system hypoxanthine/xanthine oxidase. J Biol Chem. 1989 Aug 5; 264(22):13024–8. [PubMed: 2546943]

29. Keberle H. The Biochemistry of Desferrioxamine and Its Relation to Iron Metabolism. Ann N Y Acad Sci. 1964 Oct 7.119:758–68. [PubMed: 14219455]

30. Palmer C, Roberts RL, Bero C. Deferoxamine posttreatment reduces ischemic brain injury in neonatal rats. Stroke. 1994 May; 25(5):1039–45. [PubMed: 8165675]

31. Connor JR, Menzies SL, Burdo JR, Boyer PJ. Iron and iron management proteins in neurobiology. Pediatr Neurol. 2001 Aug; 25(2):118–29. [PubMed: 11551742]

32. Wu J, Hua Y, Keep RF, Nakamura T, Hoff JT, Xi G. Iron and iron-handling proteins in the brain after intracerebral hemorrhage. Stroke. 2003 Dec; 34(12):2964–9. [PubMed: 14615611]

33. Perez de la Ossa N, Sobrino T, Silva Y, Blanco M, Millan M, Gomis M, et al. Iron-related brain damage in patients with intracerebral hemorrhage. Stroke. Apr; 41(4):810–3. [PubMed: 20185788]

34. Masuda T, Dohrmann GJ, Kwaan HC, Erickson RK, Wollman RL. Fibrinolytic activity in experimental intracerebral hematoma. J Neurosurg. 1988 Feb; 68(2):274–8. [PubMed: 3339444]

35. Yang GY, Betz AL, Chenevert TL, Brunberg JA, Hoff JT. Experimental intracerebral hemorrhage: relationship between brain edema, blood flow, and blood-brain barrier permeability in rats. J Neurosurg. 1994 Jul; 81(1):93–102. [PubMed: 8207532]

36. Naff NJ, Williams MA, Rigamonti D, Keyl PM, Hanley DF. Blood clot resolution in human cerebrospinal fluid: evidence of first-order kinetics. Neurosurgery. 2001 Sep; 49(3):614–9. discussion 9–21. [PubMed: 11523671]

37. Detraglia M, Cook FB, Stasiw DM, Cerny LC. Erythrocyte fragility in aging. Biochim Biophys Acta. 1974 Apr 29; 345(2):213–9. [PubMed: 4407524]

38. Gu Y, Hua Y, Keep RF, Morgenstern LB, Xi G. Deferoxamine reduces intracerebral hematoma-induced iron accumulation and neuronal death in piglets. Stroke. 2009 Jun; 40(6):2241–3. [PubMed: 19372448]

39. Sullivan SG, Baysal E, Stern A. Inhibition of hemin-induced hemolysis by desferrioxamine: binding of hemin to red cell membranes and the effects of alteration of membrane sulfhydryl groups. Biochim Biophys Acta. 1992 Feb 17; 1104(1):38–44. [PubMed: 1550852]

40. Franke CL, van Swieten JC, van Gijn J. Residual lesions on computed tomography after intracerebral hemorrhage. Stroke. 1991 Dec; 22(12):1530–3. [PubMed: 1962328]

41. Castillo-Ruiz MM, Campuzano O, Acarin L, Castellano B, Gonzalez B. Delayed neurodegeneration and early astrogliosis after excitotoxicity to the aged brain. Exp Gerontol. 2007 Apr; 42(4):343–54. [PubMed: 17126514]

42. Zhao X, Sun G, Zhang J, Strong R, Song W, Gonzales N, et al. Hematoma resolution as a target for intracerebral hemorrhage treatment: role for peroxisome proliferator-activated receptor gamma in microglia/macrophages. Ann Neurol. 2007 Apr; 61(4):352–62. [PubMed: 17457822]

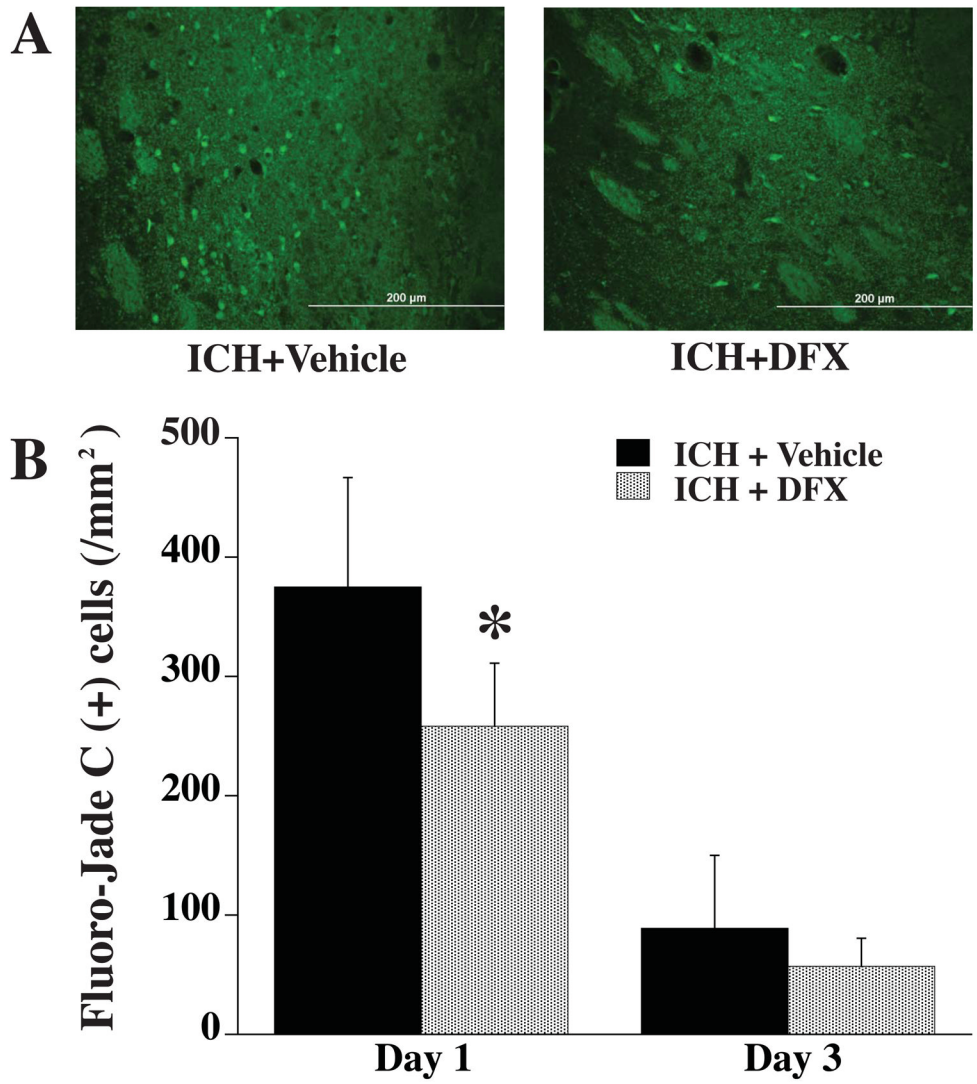

Figure 1.

A) Fluoro-Jade C positive cells in the ipsilateral basal ganglia 1 day after ICH in vehicle- and DFX-treated groups. B) Fluoro-Jade C positive cell counts in the ipsilateral basal ganglia 1 and 3 days after ICH in vehicle- and DFX-treated groups. Values are means±SD, n=5 rats per group, **P*<0.05 vs. ICH+vehicle group. Scale bar = 200 μm.

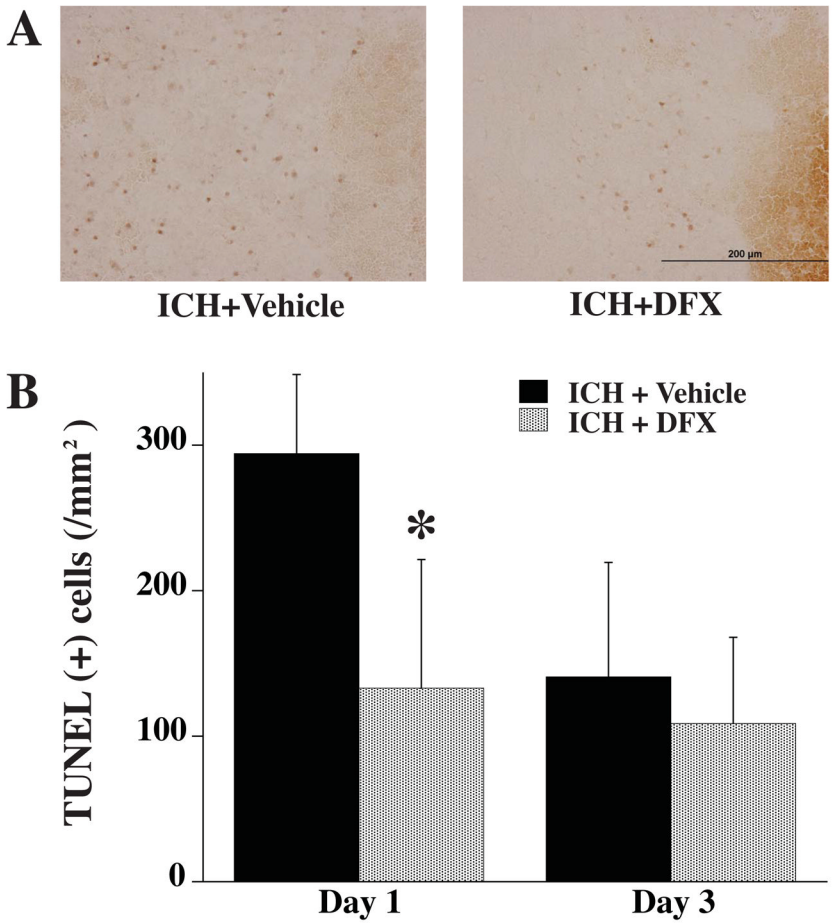

Figure 2.

A) TUNEL positive cells in the ipsilateral basal ganglia 1 day after ICH in vehicle- and DFX-treated groups. B) TUNEL positive cell counting in the ipsilateral basal ganglia 1 and 3 days after ICH in vehicle- and DFX-treated groups. Values are means±SD, n=5 rats per group, * P<0.05 vs. ICH+vehicle group. Scale bar = 200 μm.

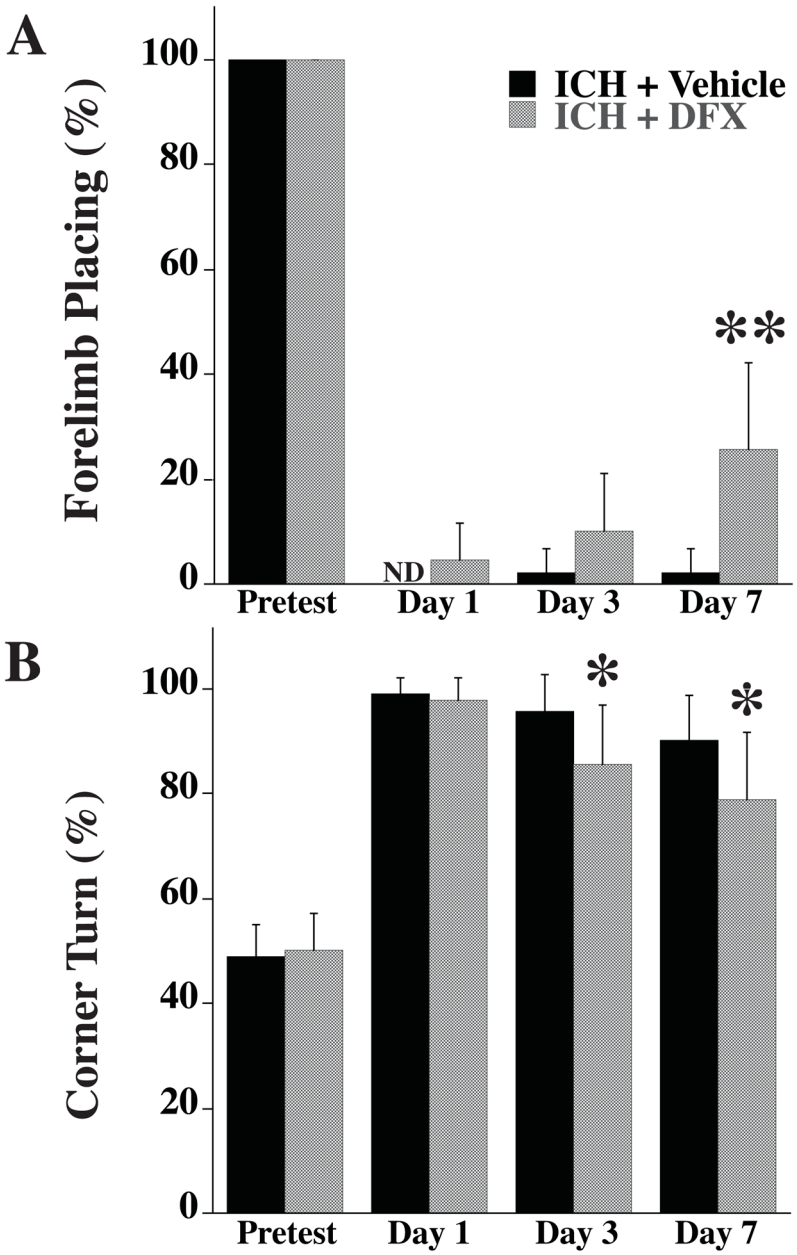

Figure 3.

Forelimb-placing (A) and corner turn (B) test scores before ICH (pretest) and 1, 3 and 7 days after ICH (ND = not detectable). Values are means±SD. n=9 rats per group, **P*<0.05 vs. ICH+vehicle group, ***P*<0.01 vs. ICH+vehicle group.

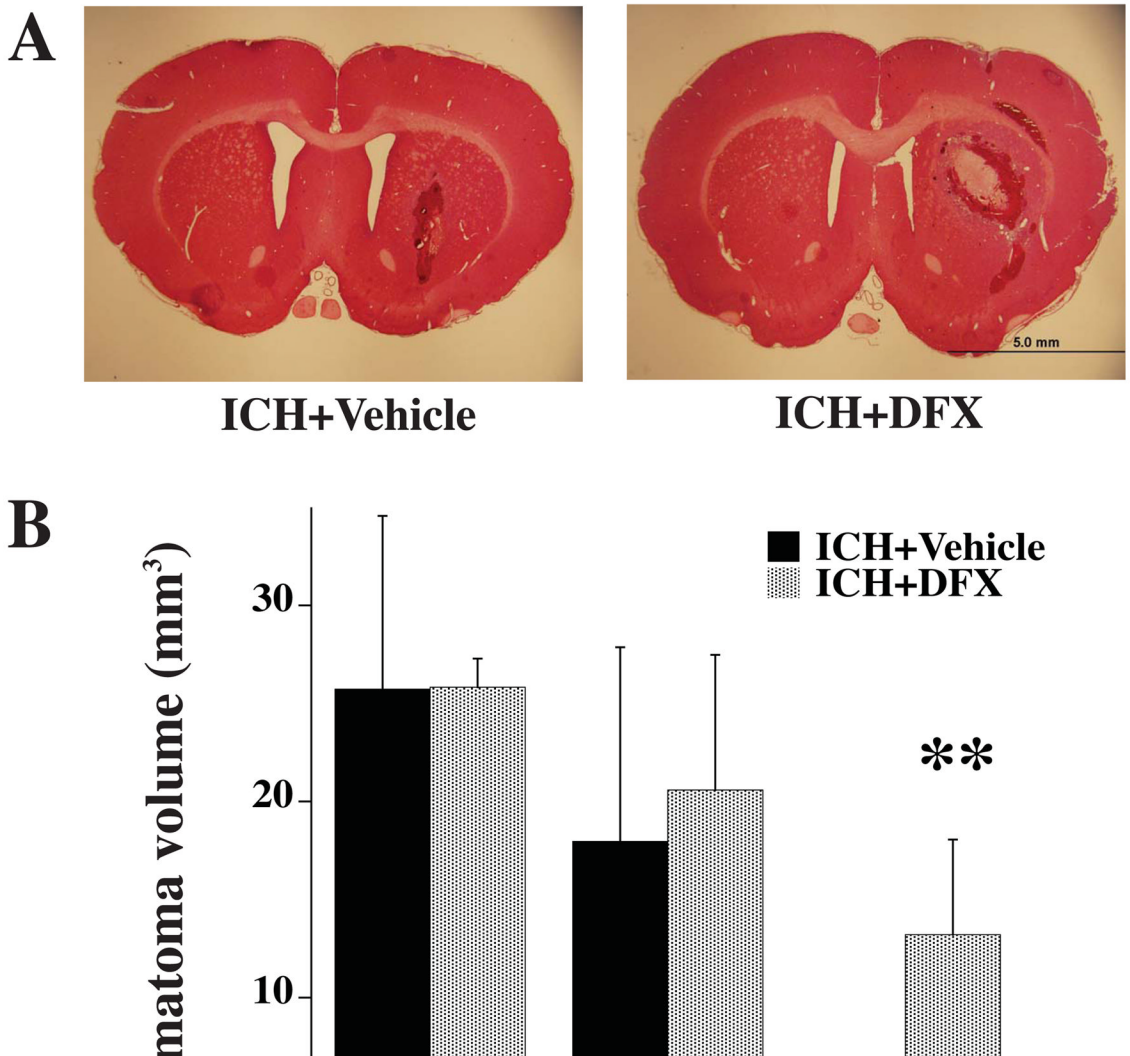

Figure 4.

A) Coronal sections (hematoxylin and eosin staining) from brains 7 days after ICH in vehicle and DFX-treated groups. B) Bar graph showing hematoma volume 1, 3 and 7 days after ICH in vehicle- and DFX-treated groups. Values are means±SD. n=4 rats per group, ** P<0.01 vs. ICH+vehicle group. Scale bar = 5.0 mm.

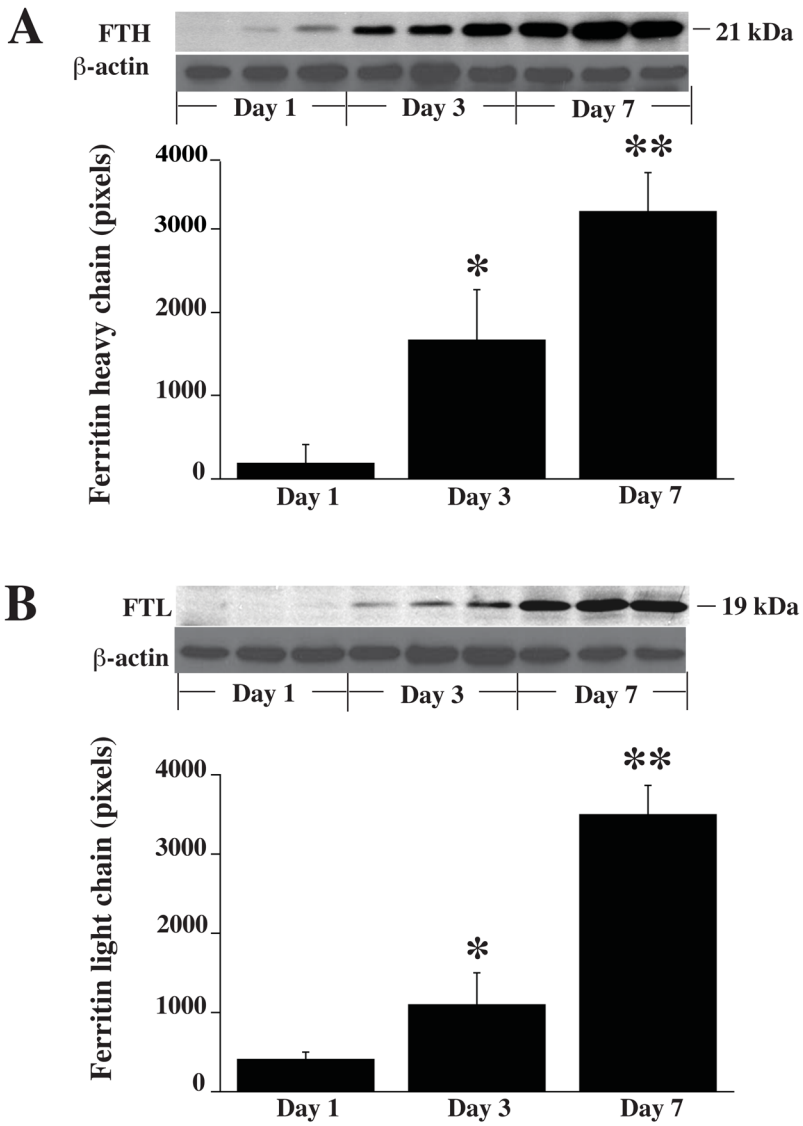

Figure 5.

A) Western blot analysis showing the time course of ferritin heavy-chain (FTH) levels in the ipsilateral basal ganglia 1, 3 and 7 days after ICH in vehicle-treated group. Bar graph quantifies the Western blotting. Beta-actin is a loading control. B) Western blot analysis showing the time course of the levels of ferritin light-chain (FTL) levels in the ipsilateral basal ganglia 1, 3 and 7 days after ICH in vehicle-treated group. Bar graph quantifies the Western blotting. Values are mean±SD, n=3 rats per group, *P<0.05 vs. ICH+vehicle group, **P<0.01 vs. ICH+vehicle group.

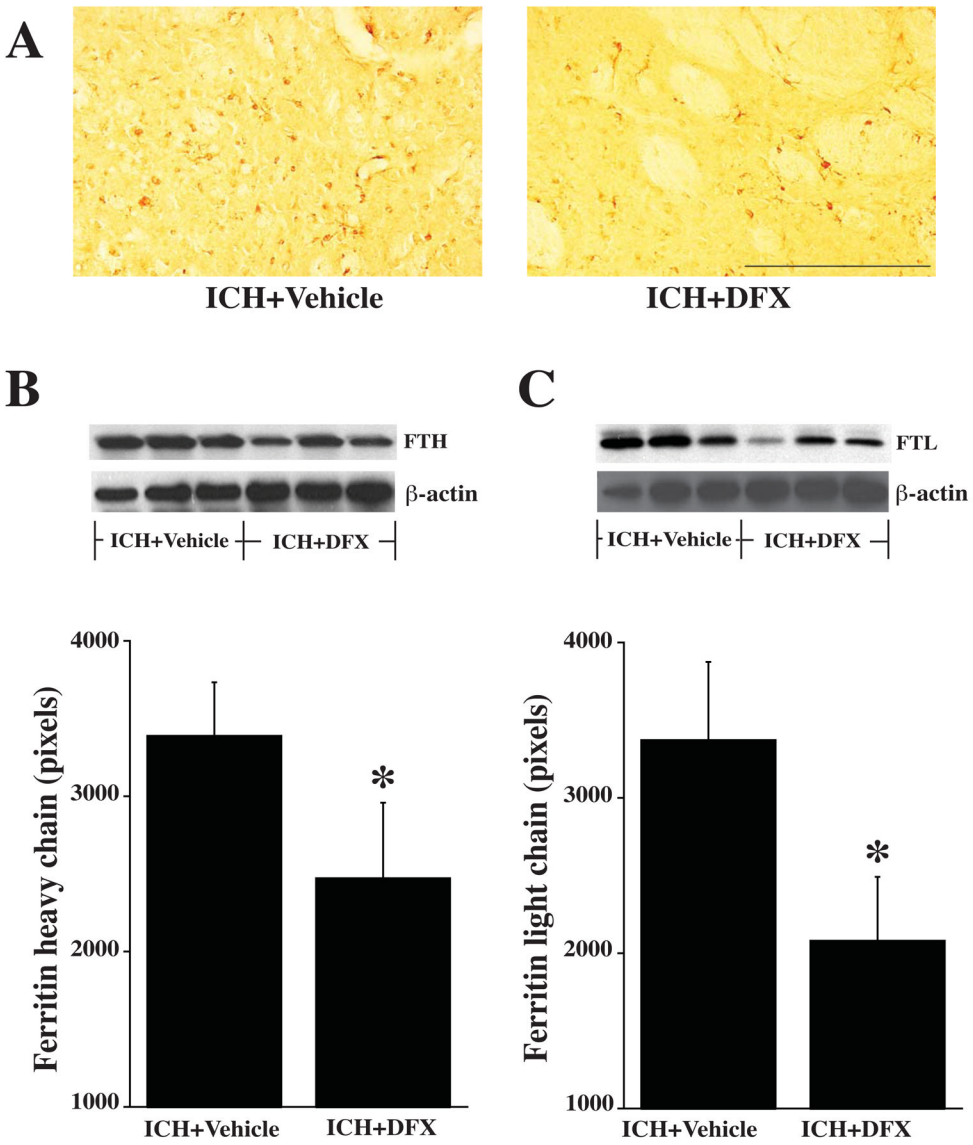

Figure 6.

A) Ferritin immunoreactivity in the ipsilateral basal ganglia 7 days after ICH in vehicle and DFX-treated rats. B) Western blot analysis showing ferritin heavy-chain levels in the ipsilateral basal ganglia 7 days after ICH in vehicle and DFX-treated groups. Bar graph quantifies the Western blotting. C) Western blot analysis showing the levels of ferritin light-chain in the ipsilateral basal ganglia 7 days after ICH in vehicle and DFX-treated groups. Bar graph quantifies the Western blotting. Values are means±SD, n=3 rats per group, **P*<0.05 vs. ICH+vehicle group. Scale bar = 200 μm.